Supporting Information

Construction of 2D@0D $InVO_4$@$MnWO_4$ S-scheme for Efficient Photocatalytic Reduction CO_2 to CO

*Wenzhuo Xiang [a], Guoyu Xu [a], Lujiang Xiao [a], Zizhong Zhang [a], Tao Ji [b], Wenyue Su [a, *]*

[a] State Key Laboratory of Photocatalysis on Energy and Environment, College of Chemistry, Fuzhou University, Fuzhou 350116, China.

[b] College of Civil Engineering, Fuzhou University, Fuzhou 350116, China.

* Corresponding author. E-mail: suweny@fzu.edu.cn.

Contents list

Experimental Section

Characterization

Powder X-ray diffraction (XRD) patterns are obtained using a Bruker D8 Advance diffractometer with Cu-Ka radiation (λ = 0.15406 nm) and a 0.02° step size. UV-vis diffuse reflectance spectra (DRS) are measured on a Varian Cary 5000 spectrophotometer, using BaSO4 as a reference. A Hitachi SU 8010 FE-SEM observes sample morphology and size. Samples for SEM are ultrasonically dispersed in deionized water, dropped onto a conductive silicon wafer, dried, and coated with gold to enhance conductivity. Transmission electron microscopy (TEM) and high-resolution TEM (HRTEM) images are captured with a FEI TECNAI G2F20 instrument. TEM samples are prepared by dispersing in ethanol, and dropping 3-5 droplets of the supernatant onto a TEM microgrid membrane to dry. SEM and TEM are conducted at 5 kV and 200 kV, respectively. X-ray photoelectron spectroscopy (XPS) and ultraviolet photoelectron spectroscopy (UPS) are performed using a Thermo ESCALAB-250 spectrometer, calibrated with 284.8 eV contaminated carbon as the standard. Low temperature N_2 and CO_2 adsorption isotherms are measured using Micromeritics ASAP 2020. Room temperature photoluminescence (PL) spectra and transient PL lifetime are measured on an Edinburgh Instrument FLS-980 spectrophotometer at 480 and 357 nm excitation wavelengths. Inductively coupled plasma atomic emission spectroscopy (ICP-AES) is performed on an Avio 200 instrument. Electron paramagnetic resonance (EPR) data are collected using a Bruker A300 spectrometer. Work functions (WF) are determined with a Kelvin probe (SKP5050, KP Technology Ltd.) using an Au-coated silicon cantilever (WF_{Au} = 5.1 eV).

The transmission path of photogenerated charges in the prepared sample are exploredbyphotoinduced redox probe experiment. Typically, using methanol and $NaIO_3$ as hole andelectronsacrificial reagents, 1 wt.% Pt and 5 wt.% PbO_2 are photodeposited on $InVO_4$@$MnWO_4$ with H_2PtCl_6 and $Pb(NO_3)_2$ as precursors, respectively.

Electrochemical measurement

PEC measurement is performed using a PAR VMP3 workstation. To prepare PEC samples, 10 mg of powder is dispersed in 450 μL DMF and 50 μL Nafion with ultrasonic dispersion. Then, 20 μL of this suspension is dropped onto a 0.28 cm^2 area on an FTO sheet and left to dry. The FTO with the sample acts as the working electrode, with Pt wire and Ag/AgCl serving as the counter and reference electrodes, respectively. Electrochemical impedance spectroscopy (EIS) is measured using a CHI-660E workstation over a frequency range of 0.1 to 100,000 Hz in a 0.5 M KCl solution containing 0.01 M $K_3[Fe(CN)_6]/K_4[Fe(CN)_6]$ (1:1). linear sweep voltammetry (LSV) curves for OER are obtained in 0.5 M KOH (pH = 13.69) at a scan rate of 10 mV s^{-1}. The photocurrent measurement is recorded in 0.2 M Na_2SO_4 (pH = 6.8) using a 300 W Xe lamp with a UV-CUT filter (λ ≥ 400 nm).

Photocatalytic H_2O oxidation half-reaction Test:

The photocatalytic H_2O oxidation half-reaction is carried out in a Pyrex top-irradiation reaction vessel connected to a glass closed gas system by dispersing 50 mg of photocatalysts power into 100 mL ultrapure water contained 0.01 M $AgNO_3$ as the sacrificial agent and 0.2 g La_2O_3 as a pH buffer agent under the irradiation of a 300 W Xe lamp with an ultraviolet cutoff filter (λ > 400 nm). The reactor is sealed and evacuated several times to eliminate the air before irradiation.

Photocatalytic CO_2 reduction half-reaction Test:

The photocatalytic CO_2 reduction half-reaction is carried out in a cylindrical glass reactor (volume, ~100 mL) by dispersing 10 mg of photocatalysts power into 10 mL acetonitrile contained 0.5 mL triethanolamine (TEOA) as sacrificial agent under the irradiation of a 300 W Xe lamp with an ultraviolet cutoff filter (λ > 400 nm). The reaction vessel is sealed and filled with CO_2 before irradiation.

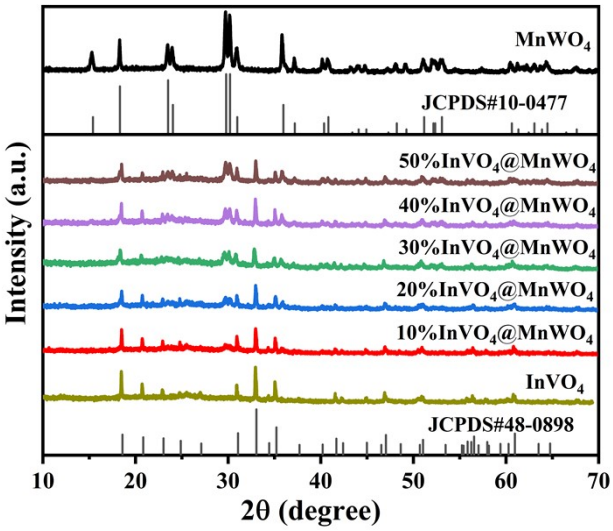

Fig. S1 XRD patterns $MnWO_4$, $InVO_4$, and a% $InVO_4$@$MnWO_4$ composites.

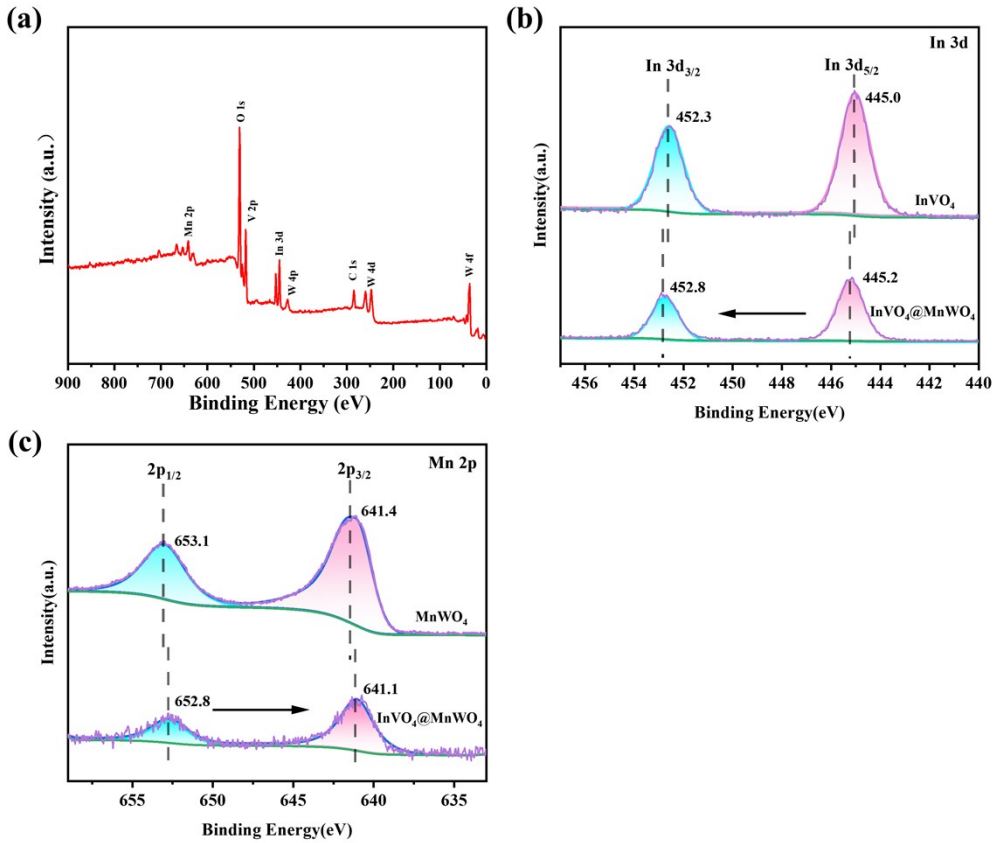

Fig. S2 XPS spectra of samples: (a) survey spectra, (b) In 3d, (c) Mn 2p.

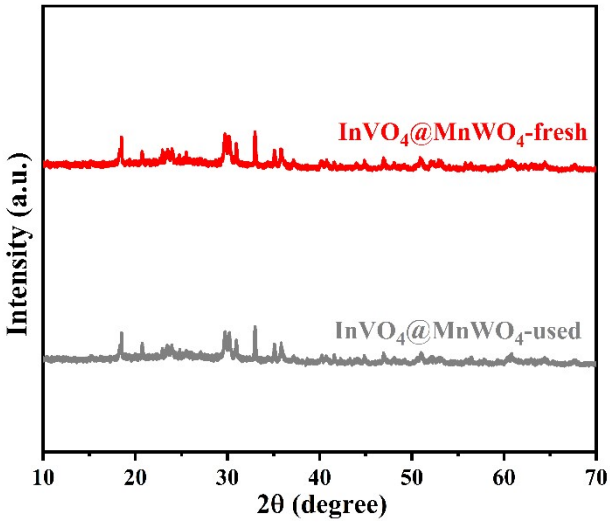

Fig. S3 XRD patterns of $InVO_4$@$MnWO_4$ composite before and after activity cycling test.

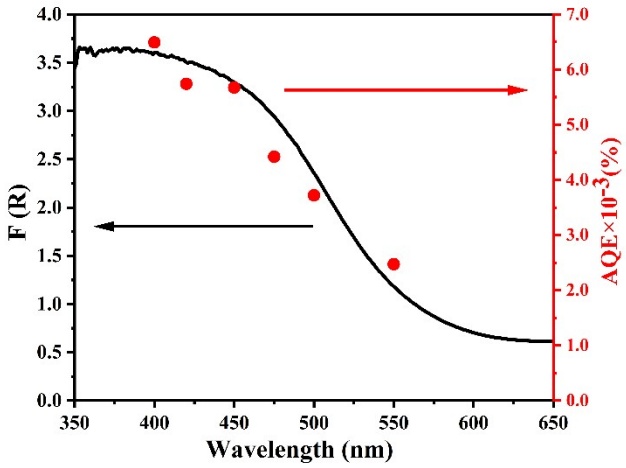

Fig. S4 The AQE wavelength-dependence of $InVO_4$@$MnWO_4$ for the photocatalytic CO_2 reduction.

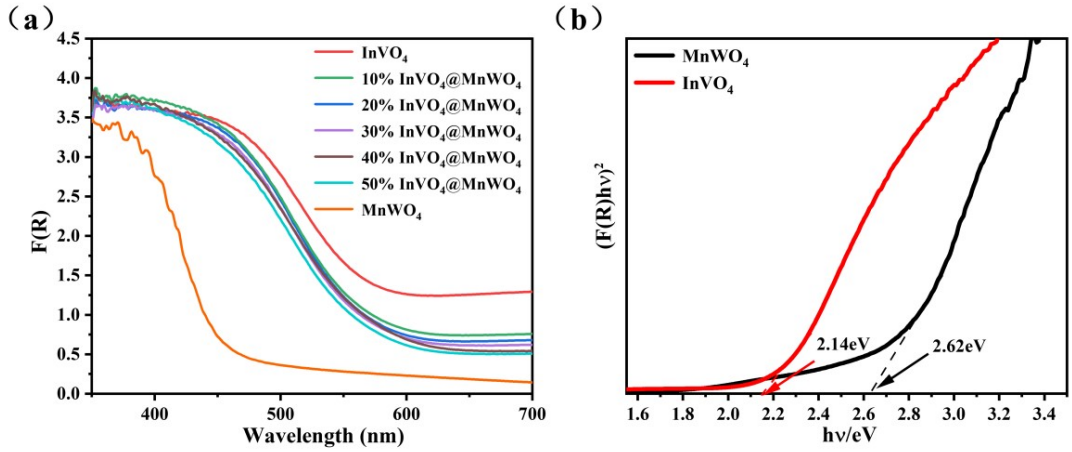

Fig. S5 (a) UV-vis DRS spectra of samples, (b) Tauc plots of $MnWO_4$ and $InVO_4$.

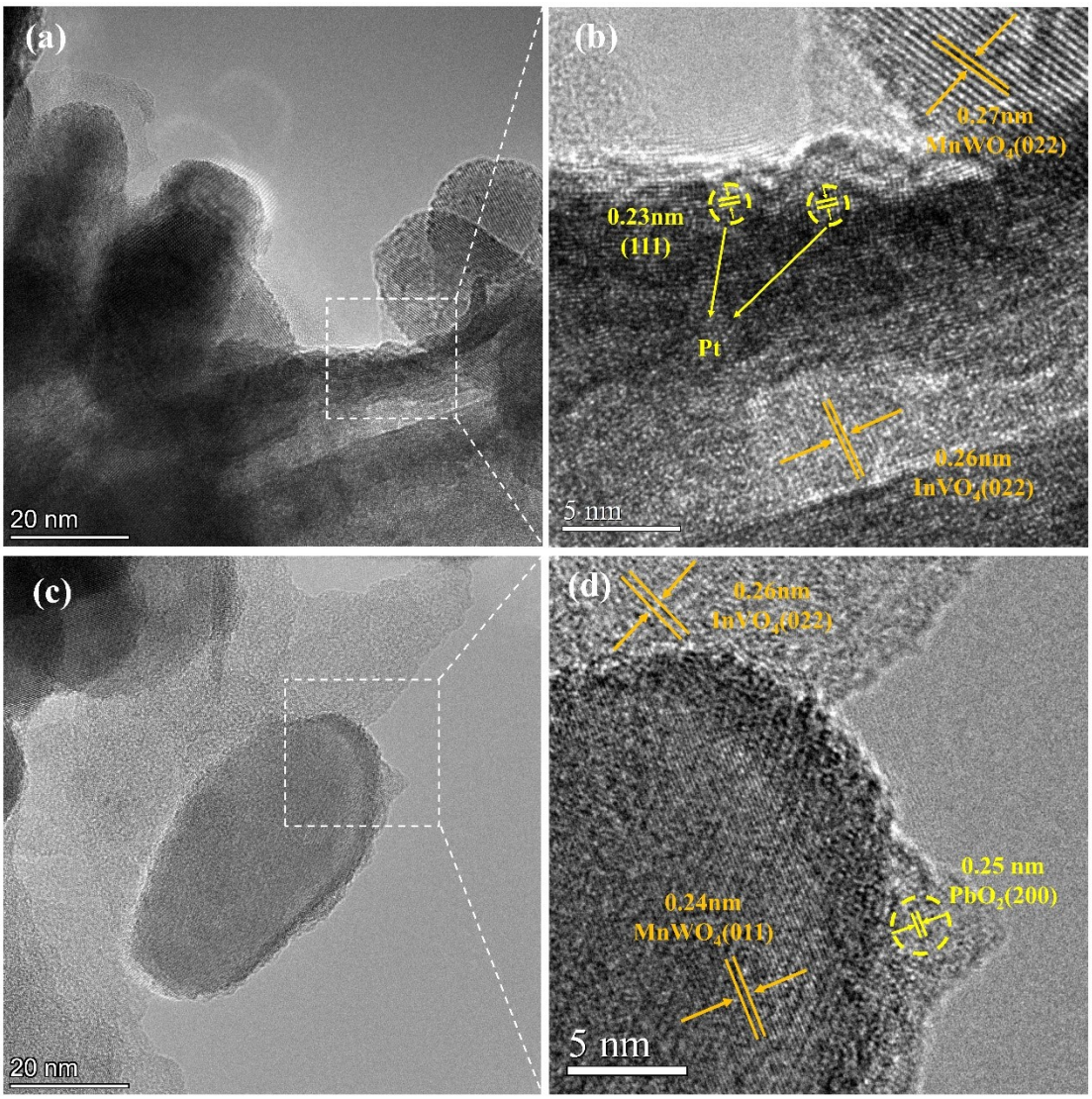

Fig. S6 TEM images of $InVO_4$@$MnWO_4$ photodeposited with Pt (a, b) nanoparticles and PbO_2（c, d）nanoparticles.

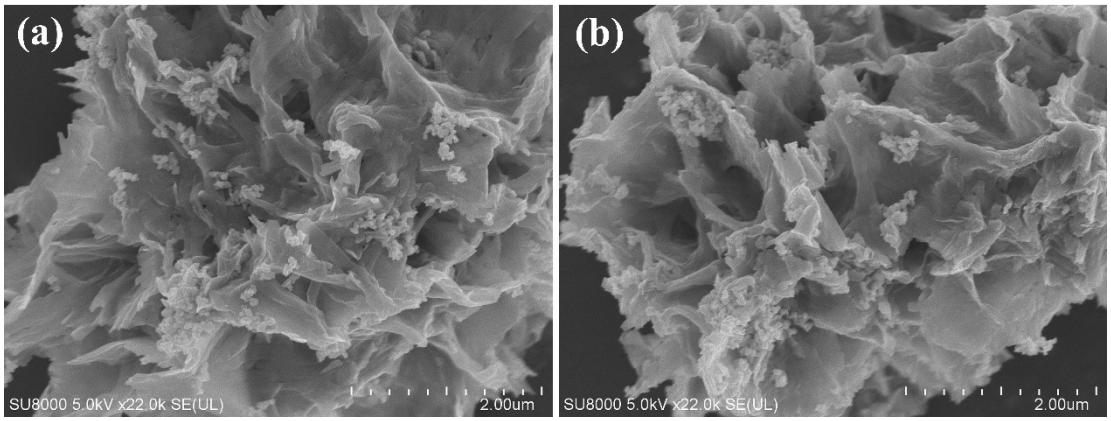

Fig. S7 SEM images of $InVO_4$@$MnWO_4$ (a) before reaction, (b) after reaction.

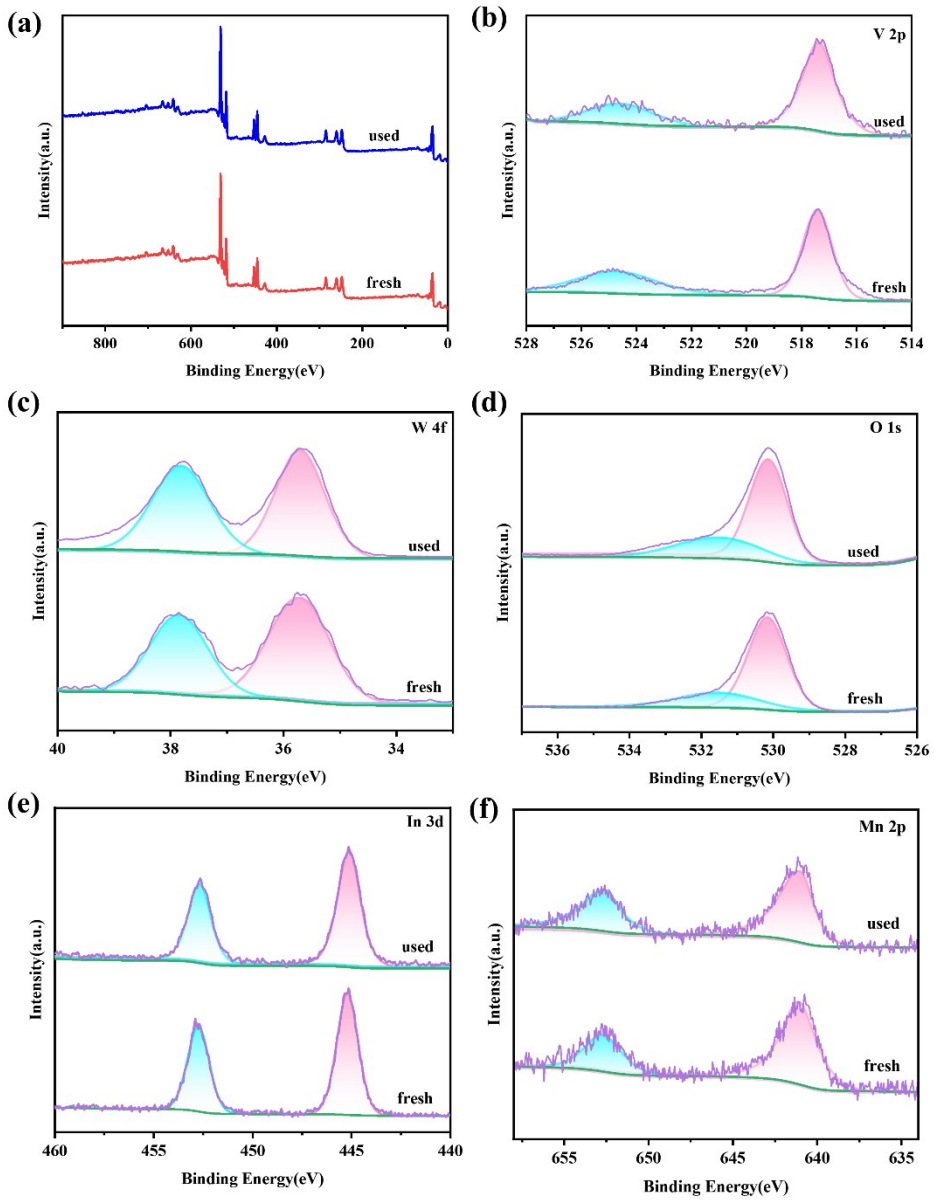

Fig. S8 XPS survey spectrum of (a) $InVO_4$@$MnWO_4$ before and after cycling tests; the high resolution XPS spectra of (b) V 2p, (c) W 4f, (d) O 1s, (e) In 3d and (f) Mn 2p.

Table S1. The W content in a% $InVO_4$@$MnWO_4$ composites.

Samples	W content (wt %)	
	Added value	Measured value
10%$InVO_4$@$MnWO_4$	6.07	5.14
20%$InVO_4$@$MnWO_4$	12.14	11.42
30%$InVO_4$@$MnWO_4$	18.21	17.63
40%$InVO_4$@$MnWO_4$	24.28	23.87
50%$InVO_4$@$MnWO_4$	30.35	29.94

Table S2. Photocatalytic CO_2 reduction performance data of $InVO_4$-based photocatalysts.

Photocatalyst	**CH_4 evolution ($\mu mol\ g^{-1}h^{-1}$)**	**CO evolution ($\mu mol\ g^{-1}h^{-1}$)**	**AQE (λ＝400nm)**	**Reference**
$InVO_4$@$MnWO_4$	-	6.20	0.0065%	This work
Bi_2WO_6/$InVO_4$	1.13	17.97	-	1
$InVO_4$/β-$AgVO_3$	1.62	12.61	0.49%	2
p-C_3N_4/$InVO_4$	1.88	14.05	-	3
$InVO_4$/$Ti_3C_2T_x$	0.09	13.83	0.0041%	4
$InVO_4$/$La_2Ti_2O_7$	-	11.7	0.002%	5

Table S3. The physical adsorption capacity of samples.

Samples	**S_{BET} (m^2/g)**	**Q_{CO2} (cm^3/g)**	**Q_{CO2}/S_{BET} (cm^3/m^2)**
$InVO_4$	15.6	4.6	0.29
$MnWO_4$	20.3	6.5	0.32
$InVO_4$@$MnWO_4$	16.9	5.6	0.33

Table S4. Exponential function fitted parameters of the TRPL decay spectra for $MnWO_4$, $InVO_4$ and $InVO_4$@$MnWO_4$ composite.

Samples	**τ_1**		**τ_2**		**τ_a**
	value (ns)	**A_1%**	**value (ns)**	**A_2%**	**value (ns)**
$InVO_4$	0.09	98.12	3.02	1.88	0.13
$MnWO_4$	0.12	99.23	3.24	0.77	0.16
$InVO_4$@$MnWO_4$	0.26	97.78	3.38	2.22	0.36

For TRPL, the decay curves can be well fitted by the following biexponential equations:

$$I_{(t)} = I_0 + A_1 \exp(-t/\tau_1) + A_2 \exp(-t/\tau_2)$$

The average carrier life of the each sample can be calculated by the following formula [6]:

$$\tau_a = (A_1\tau_1^2 + A_2\tau_2^2)/(A_1\tau_1 + A_2\tau^2)$$

where the I_0 represents the baseline correction value, A_1 and A_2 are the pre-exponential factors, and τ_1, τ_2 and τ represent the lifetime (ns) in different processes and average lifetime.

Reference

1. J. Li, W. Feng, Z. Xiu, X. Han, Direct Z-scheme charge transfer of $Bi_2WO_6/InVO_4$ interface for efficient photocatalytic CO_2 reduction, Chem. Eng. J., 2022, 446, 137129.
2. J. Yang, J. Hao, S. Xu, Q. Wang, J. Dai, A. Zhang, X. Pang, $InVO_4/\beta$-$AgVO_3$ Nanocompositeas a Direct Z-Scheme Photocatalyst toward Efficient and Selective Visible-Light-Driven CO_2 Reduction, ACS Appl. Mater. Interfaces, 2019, 11, 32025−32037.
3. L. Wang, D. Chen, S. Miao, F. Chen, C. Guo, P. Ye, J. Ning, Y. Zhong, Y. Hu, Nitricacid-assisted growth of $InVO_4$ nanobelts on protonated ultrathin C_3N_4 nanosheets as an S-scheme photocatalyst with tunable oxygen vacancies for boosting CO_2 conversion, Chem. Eng. J., 2022, 434, 133867.
4. L. Li, Y. Yang, L. Yang, X. Wang, Y. Zhou, Z. Zou, 3D Hydrangea-like $InVO_4/Ti_3C_2T_x$ Hierarchical Heterosystem Collaborating with 2D/2D Interface Interaction for Enhanced Photocatalytic CO2 Reduction, ChemNanoMat, 2021, 7, 815–823.
5. L. Xiao, L. Lin, J. Song, Z. Zhang, X. Wang, W. Su, Construction of a direct Z-scheme $InVO_4/La_2Ti_2O_7$ photocatalyst toward efficient and selective CO_2 reduction to CO, J. Alloys Compd., 2023, 935, 168086.
6. L. Yuan, Y. Li, Z. Tang, J. Gong, Y. Xu, Defect-Promoted Visible Light-Driven C-C Coupling Reactions Pairing with CO_2 Reduction, J. Catal., 2020, 390, 244-250.